types of associated leaves, to the fossil flowers.

Many characters of this early angiosperm flower illustrate the level of development of floral morphology for at least one taxon at an early time in angiosperm evolution. The pentamerous nature of all the flower parts, clear differentiation of the petals and sepals, medium size of the flowers, fused carpels and well-developed receptacular disk are generally believed to be derived floral characters (*1, 4, 25*). The free petals and stamens, bisexual nature of the flower, actinomorphy, probable entomophilous pollination, and hypogynous receptacle are generally considered "primitive" floral characters by most systematic botanists today. This mixture of characters indicates a level of floral evolution at a particular time in the history of the group. According to some hypotheses these flowers lived 15 to 20 million years after the probable latest origin (Barremian) of the angiosperms (*6–8*), thus providing time for considerable floral evolution. However, the actual evolutionary history of the group, which is evident from the considerable taxonomic diversity of mid-Cretaceous time (*14–17*), indicates great divergence early in the history of the flowering plants that cannot be easily dismissed as later evolutionary events.

The circumscription of modern plants is based primarily upon floral morphology, and the floral structure of the fossil flowers is very well known. However, assignment to a living family or order is complicated because no living flowering plant has the same floral features found in the fossil flower. This floral type is approached by members of the Saxifragales (Rosidae), Rosales (Rosidae), and Rhamnales (Rosidae). The fossil flower cannot actually be accommodated within any of these orders but it has a floral type similar to, and possibly basic in, three orders of flowering plants. This flower is of moderate size, with single, pentamerous whorls of organs borne on a very abbreviated receptacle. Its presence by mid-Cretaceous time is in agreement with the view that angiosperm evolution has not always been toward reduction and simplification, but has involved both reduction and elaboration from simple floral types (*15, 26*) as a result of coadaptive evolution with animal pollinators.

JAMES F. BASINGER*
DAVID L. DILCHER
Department of Biology, Indiana University, Bloomington 47405

References and Notes

1. A. Cronquist, *The Evolution and Classification of Flowering Plants* (Houghton-Mifflin, Boston, 1968); A. Takhtajan, *Flowering Plants—Origin and Dispersal* (Oliver and Boyd, Edinburgh, 1969); *Bot. Rev.* **46**, 225 (1980); A. Cronquist, *An Integrated System of Classification of Flowering Plants* (Columbia University Press, New York, 1981).
2. R. Thorne, *Evol. Biol.* **9**, 35 (1976).
3. R. Dahlgren, *Bot. J. Linn. Soc.* **80**, 91 (1980).
4. K. Sporne, in *The Origin and Early Evolution of the Angiosperms*, C. Beck, Ed. (Columbia Univ. Press, New York, 1976), p. 231.
5. G. L. Stebbins, *Flowering Plants, Evolution Above the Species Level* (Belknap, Cambridge, 1974); J. Walker, in *The Origin and Early Evolution of the Angiosperms*, C. Beck, Ed. (Columbia Univ. Press, New York, 1976), p. 241.
6. G. Brenner, in *The Origin and Early Evolution of the Angiosperms*, C. Beck, Ed. (Columbia Univ. Press, New York, 1976), p. 23; N. Hughes, *Palaeobiology of Angiosperm Origins* (Cambridge Univ. Press, Cambridge, 1976); N. Hughes, *Bot. Rev.* **43**, 105 (1977).
7. J. Doyle and L. Hickey, in *The Origin and Early Evolution of the Angiosperms*, C. Beck, Ed. (Columbia Univ. Press, New York, 1976), p. 139; J. Doyle, in *Patterns of Evolution in Early Angiosperms*, A. Hallam, Ed. (Elsevier, Amsterdam, 1977), p. 501.
8. L. Hickey and J. Doyle, *Bot. Rev.* **43**, (1977).
9. W. Fontaine, *U.S. Geol. Surv. Monogr. No. 15* (1889).
10. L. Lesquereux, *ibid., No. 17* (1891).
11. J. Newberry, *ibid., No. 26* (1895).
12. V. Samylina, *Bot. Zh. Leningrad* **53**, 1517 (1968).
13. J. Velenovsky, *Beitr. Palaeontol. Osterr. -Ung.* **5**, 1 (1885).
14. V. Krassilov, *Lethaia* **6**, 163 (1973).
15. D. Dilcher, *Rev. Palaeobot. Palynol.* **27**, 291 (1979).
16. V. Vakhrameev and V. Krassilov, *Paleobot. J. (Moscow)* **1**, 121 (1979).
17. G. Retallack and D. Dilcher, *Palaeontographica B* **179**, 103 (1981).
18. W. Crepet, D. Dilcher, F. Potter, *Am. J. Bot.* **62**, 813 (1975); J. Basinger, *Can. J. Bot.* **54**, 2293 (1976); W. Crepet and D. Dilcher, *Amer. J. Bot.* **64**, 714 (1977); W. Crepet, *Rev. Palaeobot. Palynol.* **25**, 241 (1978); **27**, 213 (1979); C. Daghlian, W. Crepet, T. Delevoryas, *Am. J. Bot.* **67**, 309 (1980).
19. B. Tiffney, *Nature (London)* **265**, 136 (1977); E. Friis and A. Skarby, *Ann. Bot.* **50**, 569 (1982).
20. In this report the nature and importance of this fossil flower are presented. The details concerning the relationships of the flowers are the subject of another report (D. L. Dilcher and J. F. Basinger, in preparation).
21. We thank Dr. Roger Pabian, Dr. Howard Reynolds, and Charles Beeker for help in locating and collecting the specimens.
22. R. Pabian, *Proc. Neb. Acad. Sci. (Lincoln)* **79**, 54 (1969).
23. E. Kaufman, personal communication.
24. D. Whitehead, *Evolution* **23**, 28 (1969).
25. C. Bessey, *Ann. Mo. Bot. Gard.* **2**, 109 (1915).
26. S. Carlquist, *Phytomorphology* **19**, 332 (1969); G. Gottsberger, *Plant Syst. Evol.* Suppl. **1**, 211 (1977); W. Burger, *Bot. Rev.* **43**, 345 (1977).
27. Supported by NSF grant DEB 79-10720 to D.L.D. and a Natural Sciences and Engineering Research Council of Canada Postdoctoral Fellowship to J.F.B.
* Present address: Department of Geological Sciences, University of Saskatchewan, Saskatoon, Saskatchewan, Canada S7N 0W0.

1 April 1983; accepted 6 March 1984

Magnetometry of Ingested Particles in Pulmonary Macrophages

Abstract. *Sensitive magnetometry has shown that, after inhalation of airborne magnetic dust by humans or animals, particles retained within the lungs rotate. A number of mechanisms for this rotation have been proposed, including motions of breathing, particle thermal energy, cardiac pulsations, surface fluid flows, and macrophage cytoplasmic movements. In this study the cellular mechanism was examined by magnetometry and videomicroscopy of pulmonary macrophages removed from hamster lungs 1 day after inhalation of a maghemite (γ-Fe_2O_3) aerosol. The field remaining after magnetization was measured in adherent cells and was found to decay rapidly to 30 percent of its initial magnitude within 12 minutes. The remanent-field decay rate was slowed by inhibitors of cytoplasmic motion. Videomicroscopy of pulmonary macrophages with phagocytized γ-Fe_2O_3 showed amoeboid motions that rotated the particles away from their original direction of magnetization. The results confirm that macrophage cytoplasmic movement is a primary cause of remanent-field decay in lungs and that magnetometry can be used to quantify intracellular contractile activity.*

Ferromagnetic particles can be present as contaminants in the lungs and other organs. As Cohen initially pointed out (*1*), retention in the lungs of inhaled magnetic dusts can be measured after a permanent magnetic moment in the retained particles is induced by brief application of a strong magnetic field. The combined effect of these aligned moments is to produce a remanent field that can be detected outside the body with a sensitive magnetometer. Sequential measurements have been used to determine long-term dust clearance from the lungs of smokers and nonsmokers (*2*). Cohen also noted that the magnitude of the remanent field dropped by as much as a factor of 6 during the first hour after magnetization, a phenomenon he called "relaxation." Since the particle magnetic moments are permanent and since the remanent field can be restored to its initial strength by remagnetization, Cohen attributed the relaxation to some viable process randomly rotating the magnetic particles retained in the lungs (*1*).

Cohen and others subsequently published lung clearance and relaxation curves for both humans and animals (*3, 4*). A number of speculations about the force driving relaxation have been put forward, including respiratory movements, surfactant and mucus flow, cardiac pulsations, particle diffusive motion, and cell motion. Conclusive evidence

Table 1. Results for five experimental conditions. Values are the mean ± standard deviation. Concentrations were as follows: cytochalasin D, 10 μM; nocodazole, 1 μM; dinitrophenol, 1 μM. Nocodazole and cytochalasin D were dissolved in a dimethyl sulfoxide (DMSO) vehicle at final DMSO concentrations of 0.2 to 0.3 percent. Remanent-field, decay-curve parameters for cells treated with this concentration of DMSO alone were not distinguishable from those of control cells (data not shown).

Experimental conditon	Δ (%/min)	$T_{1/2}$ (min)	B_{12} (% of B_0)
Control	39 ± 5	3.8 ± 1.6	30 ± 8
Cytochalasin D	23 ± 6	≈12	57 ± 5
Nocodazole	31 ± 6	5.5 ± 3.3	36 ± 10
4°C	6.3 ± 1	>12	84 ± 4
Dinitrophenol	13 ± 2	>12	74 ± 6

supporting a particular mechanism has been lacking. Recently, Gehr *et al.* reported this same relaxation phenomenon in hamsters after intravenous injection of magnetite (*5*). Gehr *et al.* (*5*) and Brain *et al.* (*6*) have suggested that relaxation seen in animals exposed to magnetite is due to contractions of the cytoskeleton within macrophages. Particle rotations caused by cytoplasmic rearrangements would tend to randomize the original alignment imposed by magnetization and so cause the remanent field to decrease in time. However, a clear proof of the role of cytoplasmic activity in relaxation is best sought in cells isolated from the body. This report describes magnetometric measurements and videomicroscopy of pulmonary macrophages harvested from hamsters after inhalation exposure to maghemite (γ-Fe_2O_3) aerosol.

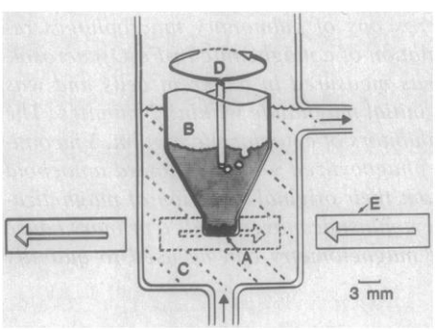

Fig. 1. Diagram of the apparatus. Cells (A) were at the bottom of a plastic vial (B) containing incubation medium that was oxygenated by a flow of air. The temperature of cells and incubation medium was maintained by a flowing water bath (C). The cells and the vial containing them were rotated about a vertical axis (D) at approximately 13 Hz. The magnetic signals from the magnetized particles within the cells were sensed by an arrangement of four flux-gate probes (E), two of which pointed to the left as shown, and two of which pointed to the right and were situated above and below the plane of this figure (dotted outline). With this configuration, the probes are maximally sensitive to the dipole magnetic field from the cells and magnetic noise from outside sources is effectively canceled. Electronic processing of the magnetometer output utilized lock-in detection of only those signals in phase with sample rotation.

Pulmonary macrophages are part of a system of mononuclear phagocytic cells found widely scattered in body tissues (*7*). These lung cells reside on alveolar surfaces and avidly ingest particles deposited there from inhaled air (*8*). Within 1 day of a short-term aerosol exposure, the majority of retained particles are found within phagosomes or secondary lysosomes of pulmonary macrophages (*9*). Pulmonary macrophages containing magnetic particles were obtained by having unanesthetized hamsters breathe a maghemite aerosol (aerodynamic diameter, 0.7 μm) for 1/2 hour (*10*). Twenty hours after inhalation exposure, pulmonary macrophages were harvested by means of multiple saline washings of the lung (*11*). Cell recovery for eight hamsters ranged from (2 to 8) × 10^6 macrophages per animal; the amount of phagocytized dust was 15 to 75 μg of γ-Fe_2O_3 per animal. Cells were resuspended in Hanks medium supplemented with 0.2 percent bovine serum albumin and 20 mM Hepes buffer (pH = 7.3 at 37°C), were centrifuged onto the bottom of plastic vials, and were allowed to adhere for 1/2 hour at 37°C. The attached macrophages could not rotate freely, and thus the intracellular particles were ready for magnetometric study.

The macrophages from each hamster were divided into separate portions, which were incubated for an additional 1/2 hour under one of the following conditions: (i) 37°C, control; (ii) 37°C and 10 μM cytochalasin D (cytD); (iii) 37°C and 1 μM nocodazole; (iv) 4°C; (v) 37°C and 1 mM dinitrophenol (DNP); and (vi) 37°C and 10 percent Formalin.

Alignment of the ingested-particle magnetic moments was produced by 2-minute application of a strong uniform field (0.1 tesla = 10^3 G). After removal of this field, the particles produced a weak remanent magnetic field of about 4 nT at 2 cm from the cells, corresponding to about 0.01 ng of maghemite per cell. By the use of noise-reduction and signal-enhancement techniques, the cell magnetic field was measured in the presence of much larger background fields [Earth's field (~ 10^4 nT) and fluctuating magnetic sources in the environment (~ 10^2 nT)]. One layer of magnetic shielding was used in conjunction with a sensitive flux-gate magnetometer (*12*). Phase-sensitive signal detection further improved the signal-to-noise ratio. The cell vial was rotated in the center of the probe array, and only magnetic field signals that were in synchrony with sample rotation were detected and amplified. The positions of cells and magnetometer probes are depicted in Fig. 1. Cell temperature was controlled by a circulating water bath; oxygenation was maintained by bubbling air through the incubation medium. The rotating portion of the apparatus was air-driven and constructed of nonmetallic materials to avoid spurious magnetic signals synchronized to the rotation rate.

Figure 2 shows recordings of the magnetic field from the cells. If cells were Formalin-fixed, the remanent field was constant (Fig. 2, curve A). However, for oxygenated macrophages at 37°C, the field decreased rapidly (Fig. 2, curve D), so that only 30 percent of its initial magnitude remained after 12 minutes. The decrease is due to random rotation of particles away from their original direction of magnetization. This result confirms that the relaxation phenomenon can occur in isolated macrophages. Rotations of endosomes can be produced

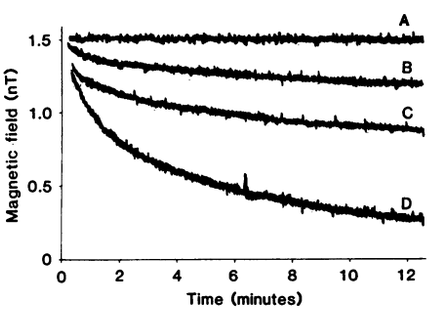

Fig. 2. Recorded magnetometer output shows the decay of the remanent field after magnetization. Zero time on this graph represents the instant at which the cells were removed from the magnetizing field and placed in the measurement apparatus. The decay of the remanent field is dramatically influenced by the functional state of the cells. Formalin-fixed cells exhibited a constant remanent field (curve A). Viable cells oxygenated at 37°C revealed their cellular movements by a rapid decay in the remanent field (curve D). The cellular movements could be inhibited and the decay slowed by 10 μM cytD (curve C), by incubation at 4°C (curve B), or by other agents (see Table 1).

by cytoplasmic streaming where such flow has a shear component. The remanent field could be restored to its initial magnitude by remagnetization, an indication that neither particles nor particle-laden cells were being lost from the observation region.

The remanent-field decay was influenced by modifications of cell function. When macrophages were cooled to 4°C (Fig. 2, curve B), the decrease of the remanent magnetic field was markedly slowed, an indication that cellular processes moving and rotating the particles were impaired. The force for cellular motility is thought to be generated by the interaction of filaments of actin with myosin. It is known that cytD interferes with the organization of actin filaments and prevents gelation of actomyosin extracts when present at concentrations greater than 5 μM (*13*). Cells incubated with cytD produced lower decay rates for the remanent field (Fig. 2, curve C) than control cells (Fig. 2, curve D).

The decay curves of the remanent field were not pure exponentials and so were characterized by three parameters: Δ, the decay rate at time $t = 0$ (percentage per minute); $T_{1/2}$, the time required for the remanent field to reach half its initial amplitude; and B_{12}, the percentage of the initial field (B_0) remaining at 12 minutes. Results for five experimental conditions are summarized in Table 1. Nocodazole, an agent that causes microtubule disassembly (*14*), reduced the decay rate but to a lesser degree than cytD. This difference may be due to the fact that microtubules are thought to guide cellular motions rather than generate force. Since DNP inhibits oxidative phosphorylation, it would be expected to restrict the amount of adenosine triphosphate available for cytoplasmic movement. Incubation with DNP reduced remanent field decay more than with the two other inhibitors but less than the 4°C conditions (Table 1). The data in Table 1 are consistent with the interpretation that the decay rate of the remanent magnetic field is closely linked to the functional ability of the cell to maintain general contractile activity.

Samples of cells with particle-containing phagosomes were examined by electron microscopy and time-lapse videomicroscopy. Transmission electron micrographs showed maghemite particles to be intracellular and located within phagosomes or secondary lysosomes (Fig. 3A). The iron oxide could also be resolved in living cells under bright-field or phase-contrast conditions because of its brown pigmentation (Fig. 3B). Use of a Zeiss Planapo ×63 objective with 1.4 aperture allowed optical sectioning of cells so that the intracellular location of maghemite particles could be appreciated. When a magnetic field was applied, the alignment of particles within cells could be clearly seen (Fig. 3C). Compression of time by a factor of 9 through the use of time-lapse video showed pseudopod formation and retraction, veil movement from periphery to center, cytoplasmic rearrangements, and the inclusion of maghemite-containing endosomes in this general motion (*15*). Active surface membrane ruffling was also observed in macrophages by Nomarski differential-interference contrast (Fig. 3D). Cells treated with cytD exhibited markedly reduced cytoplasmic activity. Nocodazole-treated cells were more active than cytD-treated cells, but the motion was confined to a single cytoplasmic extension that moved randomly about the cell border. Formalin-fixed cells showed no motion. These time-lapse video observations confirmed that the remanent-field decay phenomenon was associated with motions of the macrophage cytoplasm which reoriented the alignment of intracellular maghemite particles.

These results are important in relation to studies of ferromagnetic contaminants within intact organisms (*1–6*). Cytoplasmic motions have been implicated as a cause of remanent-field decay. However, mechanisms such as ciliary beating, cardiovascular pulsations, surfactant secretion, gastrointestinal motility, Brownian movement, and ventilatory motions needed to be considered. On the basis of the correlation of videomicroscopy and magnetometry of isolated pulmonary marcophages reported here, it is possible to state that the relaxation phenomenon can occur in the complete absence of tissue movements and for a clearly delineated cell type. Since the rate of relaxation in macrophages is quantitatively similar to that seen in animals and humans, it further appears that part of the

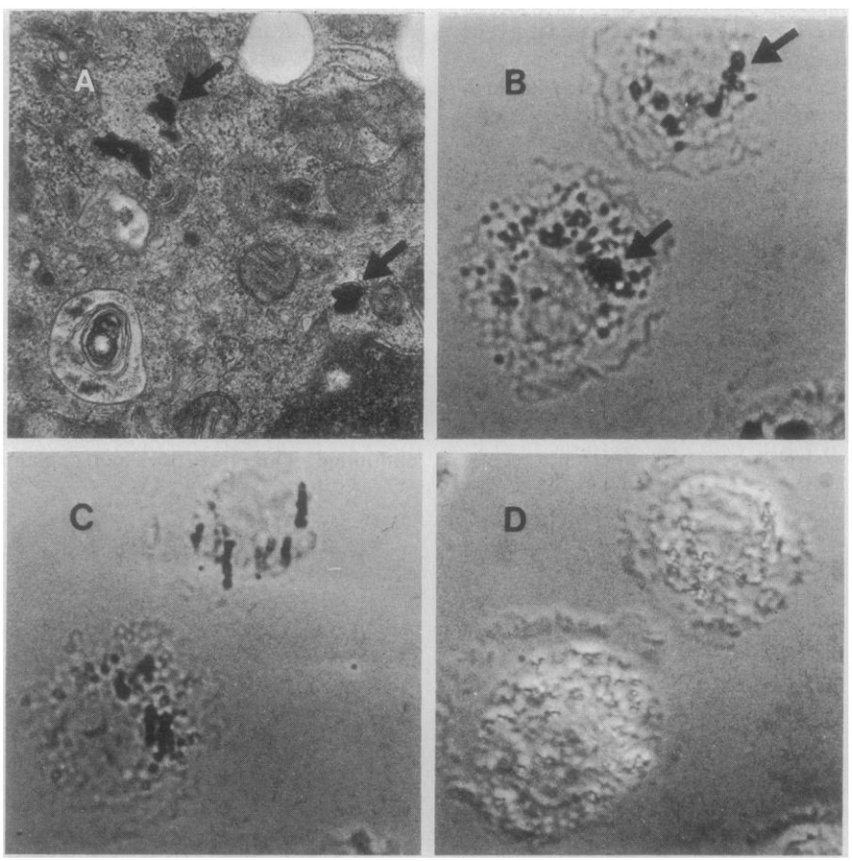

Fig. 3. Pulmonary macrophages isolated from hamsters. Pulmonary macrophages ingested maghemite particles deposited on lung surfaces after inhalation. After in vivo phagocytosis, macrophages were harvested by lung lavage. Electron micrograph (A) shows the electron-dense maghemite to be intracellular within membrane-bound vesicles (arrows) (×34,000). Particles could be identified by their brownish pigmentation, seen as dark objects (arrows) in monochrome light micrographs (B and C) (×1800). Application of a 50-mT magnetizing field produced an alignment that could be appreciated visually (C). Time-lapse video observations based on the use of both Nomarski (D) and phase-contrast techniques showed cytoplasmic motions that rotated particle-containing phagosomes and randomized the alignment achieved by magnetization (×1800).

remanent magnetic field decay observed in vivo can be attributed to intracellular motions within particle-containing macrophages.

Magnetometry can also be used in the study of cytoskeletal function and intracellular viscosity. Frey-Wyssling pointed out as early as 1938 that subcellular structures appear to be attached to each other by protoplasmic threads (*16*), and more recent data support the idea that the cytoplasm is a highly organized lattice of elements (*17*). The mechanisms responsible for cell organelle movement in motile nonmuscle cells is currently under close scrutiny (*13, 14, 18*), and the role of various cytoplasmic filaments has not been settled. With magnetometric techniques it is possible to detect noninvasively the motion of magnetic particles within isolated cells, and also external magnetic fields can be used to twist the particles and probe their viscous environment (*19*). Although intracellular particle motions can be observed in videomicroscopy on a cell-by-cell basis, magnetometric techniques provide a quantitative description of mechanical events and cytoplasmic motility within a large ensemble of cells. Thus, measurement and manipulation of magnetic particles within cells in vitro or in situ can be used to sense amoeboid motions, to probe cell rheology, and to assess the integrity of contractile elements.

PETER A. VALBERG
Department of Environmental Science and Physiology, Harvard School of Public Health, Boston, Massachusetts 02115

References and Notes

1. D. Cohen, *Science* **180**, 745 (1973).
2. _____, S. F. Arai, J. D. Brain, *ibid.* **204**, 514 (1979).
3. D. Cohen, *IEEE Trans. Magn.* **MAG-11**, 694 (1975); P.-L. Kalliomäki *et al.*, *Scand. J. Work Environ. Health* **4**, 232 (1976); *Int. Arch. Occup. Environ. Health* **43**, 85 (1979); D. Cohen, T. S. Crowther, G. W. Gibbs, M. R. Becklake, *Environ. Res.* **26**, 535 (1981); M. Halpern *et al.*, *Exp. Lung Res.* **2**, 27 (1981); A. P. Freedman, S. E. Robinson, F. H. Y. Green, *Ann. Occup. Hyg.* **26**, 319 (1982); D. Cohen, I. Nemoto, S. Arai, *IEEE Trans. Biomed. Eng.*, in press.
4. P. A. Valberg and J. D. Brain, *Am. Rev. Respir. Dis.* **120**, 1013 (1979).
5. P. Gehr, J. D. Brain, S. B. Bloom, P. A. Valberg, *Nature (London)* **302**, 336 (1983).
6. J. D. Brain, S. B. Bloom, P. A. Valberg, P. Gehr, *Exp. Lung Res.*, in press; P. Gehr, J. D. Brain, I. Nemoto, S. B. Bloom, *J. Appl. Physiol. Respir. Environ. Exercise Physiol.* **55**, 1196 (1983).
7. R. VanFurth, Ed., *Mononuclear Phagocytes: Functional Aspects* (Nijhoff, The Hague, 1980).
8. G. M. Green and E. H. Kass, *J. Exp. Med.* **119**, 167 (1964); G. M. Green, *Arch. Intern. Med.* **131**, 109 (1973); S. C. Silverstein *et al.*, *Annu. Rev. Biochem.* **46**, 669 (1977); W. G. Hocking and D. W. Golde, *N. Engl. J. Med.* **301**, 580 (1979); *ibid.*, p. 639; R. M. Steinman *et al.*, *J. Cell. Biol.* **96**, 1 (1983).
9. S. P. Sorokin and J. D. Brain, *Anat. Rec.* **175**, 448 (1973).
10. A maghemite (γ-Fe_2O_3) aerosol was produced by the controlled combustion of iron pentacarbonyl. The particles produced are crystalline in appearance and about 0.1 to 0.2 μm in diameter (*4*).
11. Each hamster was anesthetized, and the trachea was exposed and cannulated. The lungs were lavaged 13 times with Dulbecco's calcium- and magnesium-free phosphate-buffered saline (4 ml per wash). The absence of divalent cations promotes detachment of macrophages from the alveolar surface, and gentle massage of the chest further increases the cell yield [P. A. Valberg *et al.*, *Exp. Cell Res.* **141**, 1 (1982)].
12. The remanent magnetic field was sensed with a Förster (model 1.107) flux-gate magnetometer with two sets of special field and gradient probes wired in a second-order gradiometer configuration (see Fig. 1). The probes were oriented parallel to field lines from the local magnetic dipole to optimize their sensitivity to the field from the cells (the signals from the probes were added to give four times the signal from one probe) and to strongly reject the more uniform fields from distant sources. The output from this instrument was sent to a phase-sensitive amplifier, where it was combined with a reference signal synchronized to cell cuvette rotation.
13. S. J. Atlas and S. Lin, *J. Cell Biol.* **76**, 360 (1978); T. D. Pollard, *ibid.* **91**, 156s (1981); M. P. Sheetz and J. A. Spudich, *Nature (London)* **303**, 31 (1983).
14. M. J. DeBrabander *et al.*, *Cancer Res.* **36**, 905 (1976); B. Herman and D. F. Albertini, *Cell Motility* **2**, 583 (1982).
15. Unstained macrophages maintained in Hanks medium at 37°C were examined in a chamber under a Zeiss Photoscope III. Video recording utilized a Venus camera (model DV2) and a Panasonic time-lapse videotape recorder (model NV-8030). Time and date were automatically combined with the image (RCA TC1440B).
16. A. Frey-Wyssling, *Submikroskopische Morphologie des Protoplasmas und seiner Derivate* (Bontraeger, Berlin, 1938).
17. J. J. Wolosewick and K. R. Porter, *J. Cell. Biol.* **82**, 114 (1979); J. H. M. Temmink and J. Spiele, *J. Cell Sci.* **41**, 19 (1980).
18. T. Pollard and S. Ito, *J. Cell Biol.* **46**, 267 (1970); E. P. Reaven and S. G. Axline, *ibid.* **59**, 12 (1973); R. D. Goldman *et al.*, *Annu. Rev. Physiol.* **41**, 703 (1979); D. L. Taylor and J. S. Condeelis, *Int. Rev. Cytol.* **56**, 57 (1979); M. C. Beckerle and K. R. Porter, *J. Cell Biol.* **96**, 354 (1983).
19. F. H. C. Crick and A. F. W. Hughes, *Exp. Cell Res.* **1**, 37 (1950); K. Yagi, *Comp. Biochem. Physiol.* **3**, 73 (1961); A. Heilbronn, *Jahrb. Wiss. Bot.* **61**, 284 (1922); M. Sato, T. Z. Wong, R. D. Allen, *J. Cell Biol.* **97**, 1089 (1983).
20. I thank D. Albertini, J. Brain, D. Cohen, P. Gehr, and B. Herman for help and advice; R. Stearns for producing the electron micrograph; and S. Bloom for assisting with the aerosol exposures. Research supported by NIH grants HL-29175 and ES-00002.

18 July 1983; accepted 22 February 1984

Anatomically Distinct Opiate Receptor Fields Mediate Reward and Physical Dependence

Abstract. *Rats never before exposed to opioids rapidly learned to press a lever for microinjections of morphine into the ventral tegmental area. Challenge by a narcotic antagonist produced no signs of physical dependence. Dependence was not seen after long-term morphine infusions into the ventral tegmentum but was seen after similar infusions into the periventricular gray region. Thus a major rewarding property of morphine is independent of the drug's ability to produce physical dependence. These data challenge models of drug addiction that propose physical dependence as necessary for the rewarding effects of opioids.*

The rewarding effects of opioid injections in humans and laboratory animals (*1*) have been presumed by many investigators (*2*) to result from the ability of opioids to relieve the distress of withdrawal after long-term drug use is discontinued. This view does not explain, however, why opioids are initially taken or why they retain their potent rewarding effects after long periods of drug abstinence. Several workers (*3*) have argued that opioids can be rewarding independent of any ability to alleviate withdrawal stress, but in most demonstrations of opioid reward, repeated injections are given and some degree of dependence may play a role (*4*). We now report that opioids can be rewarding even when they are restricted to brain regions where they do not activate mechanisms involved in physical dependence. Nondependent rats learned to press a lever for morphine injections into the ventral tegmental area but not into the periventricular gray region; rats were made physically dependent on morphine by long-term infusions into the periventricular gray but not by infusions restricted to the ventral tegmental area.

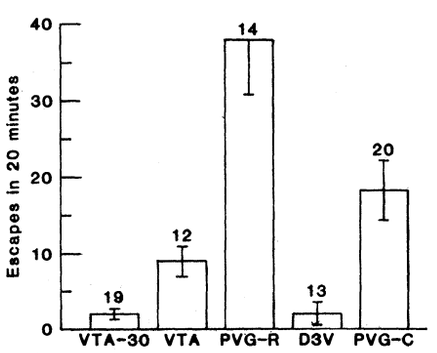

Fig. 1. Naloxone-precipitated escape responding after long-term morphine infusions into various brain regions. Abbreviations: *VTA-30*, ventral tegmental area with angled cannulas; *VTA*, ventral tegmental area with unangled cannulas; *PVG-R*, rostral aspect of the periventricular gray substance; *D3V*, dorsal aspect of the third ventricle; and *PVG-C*, caudal aspect of the periventricular gray substance. Error bars depict standard errors of the means. The number of subjects is shown above each bar.

To identify the opiate receptor fields involved in opioid reward and physical dependence, we microinjected morphine directly into brain tissue. Experimentally naïve rats learned to administer 100-ng infusions of morphine sulfate into the ventral tegmental area (*5*) but failed to learn to press for the same infusions into other opiate receptor fields (*6*). To deter-